

## Calculation of elastic constants in defected and amorphous silicon by quantum simulations

G. De Sandre

*Istituto Nazionale per la Fisica della Materia and Dipartimento di Fisica, Università di Milano via Celoria 16, I-20133 Milano, Italy  
and Istituto Nazionale per la Fisica della Materia and Dipartimento di Ingegneria Nucleare,  
Politecnico di Milano via Ponzio 34/3, I-20133 Milano, Italy*

L. Colombo

*Istituto Nazionale per la Fisica della Materia and Dipartimento di Fisica, Università di Milano via Celoria 16, I-20133 Milano, Italy*

C. Bottani

*Istituto Nazionale per la Fisica della Materia and Dipartimento di Ingegneria Nucleare, Politecnico di Milano via Ponzio 34/3,  
I-20133 Milano, Italy*

(Received 15 March 1996)

We present a quantum-mechanical calculation of finite-temperature elastic constants in silicon based on tight-binding molecular dynamics. We investigate amorphous silicon as obtained from the melt, and the evolution of elastic constants in silicon during ion implantation. The effect of post-implantation thermal annealing is also presented and discussed. [S0163-1829(96)05438-0]

Among several other thermodynamical response functions, elastic constants (EC's) play a special role in semiconductor materials science. They are, in fact, almost routinely measured and used to characterize the mechanical and structural properties of semiconductors.<sup>1,2</sup> Moreover, the monitoring of EC's is a valuable tool to control the effects of materials processing. Therefore the accurate and efficient calculation of EC's is a basic issue to understand the behavior of materials.

In this area two different theoretical approaches are currently used: (i) static total-energy methods for a zero-temperature calculation of elastic constants<sup>3-5</sup> and (ii) molecular-dynamics (MD) simulations where EC's are evaluated at finite temperature (dynamic calculations).<sup>6</sup> The first approach can be straightforwardly followed within an *ab initio* framework and provides a rather accurate prediction of the elastic properties of the selected material. On the other hand, the dynamic calculations allow for the evaluation of both isothermal and adiabatic EC's at any temperature. The limitation of such methods is that the numerical convergence of the fluctuation formulas<sup>6</sup> needed to compute EC's is slow and quite long simulation times have to be used. So far, this feature made the implementation of a numerical computation of EC's affordable only within classical MD based on empirical potentials.<sup>7,8</sup> The EC's of both crystalline (*c*-Si) and (*a*-Si) silicon have been in fact determined by means of numerical simulations.<sup>9,10</sup> Fully empirical classical potential, however, have some important well-known limitations due to their reduced transferability. In particular, they can hardly concern defected materials where quantum-mechanical phenomena (like those occurring, for instance, during ion-beam implantation or radiation damage) affect the chemical bonding.

In this work we present a theoretical investigation addressed to compute finite-temperature EC's of a disordered material on a quantum-mechanical basis. Our main goal is to prove the feasibility of such a project and to provide a show-

case application to amorphous and defected silicon. In order to overcome the limitations discussed above, we apply the general theory for the calculation of elastic constants by computer simulation<sup>11</sup> to a quantum-mechanical scheme, namely, the semiempirical tight-binding molecular dynamics (TBMD).

TBMD is an accurate and efficient quantum-mechanical simulation method<sup>12</sup> which has been successfully used to investigate the structural and electronic properties of *a*-Si as obtained both by quenching from the melt<sup>13</sup> and by ion implantation.<sup>14</sup> Within the TBMD formulation the total potential energy  $U$  of a system of  $N$  atoms is given by

$$U = 2 \sum_n^{(\text{occupied})} \langle \Psi_n | \hat{H}_{\text{TB}} | \Psi_n \rangle + U_{\text{rep}}(\{\mathbf{x}_\alpha\}), \quad (1)$$

where  $|\Psi_n\rangle$  is the eigenfunction of the one-electron tight-binding (TB) Hamiltonian  $\hat{H}_{\text{TB}}$  corresponding to the  $n$ th eigenvalue and  $\mathbf{x}_\alpha$  is the position vector of the  $\alpha$ th atom. The first contribution represents the band structure energy calculated from a semiempirical orthogonal TB parametrization, and the last term is the short-range repulsive energy.<sup>12</sup> It is clear from Eq. (1) that, because of the former contribution, the interatomic forces  $\mathbf{f}_\alpha = -\partial U / \partial \mathbf{x}_\alpha$  are many body in nature and, therefore, a suitable formulation for the calculation of EC's not limited to pairwise potentials is needed.

It is easy to prove that Eq. (1) can be cast in the form

$$U = \sum_{\alpha,\beta} \varphi(\mathbf{x}_{\alpha\beta}), \quad (2)$$

where  $\varphi(\mathbf{x}_{\alpha\beta})$  is an effective potential (incorporating both the band structure and the repulsive contributions) depending on the distance vector  $\mathbf{x}_{\alpha\beta} = \mathbf{x}_\alpha - \mathbf{x}_\beta$  of any atom pair in the simulation box. The  $C_{ijkl}$  component of the isothermal elastic tensor is defined as the derivative of the stress tensor  $\tau_{ij}$

TABLE I. Room-temperature elastic constants (units of GPa) of *c*-Si and *a*-Si. TBMD results are obtained with a 64-atom simulation box.

		$C_{11}$	$C_{12}$	$C_{44}$
<i>c</i> -Si	Expt. from Ref. 6	166	64	79.6
<i>a</i> -Si	Expt. from Refs. 15–17	156	58.4	48.8
<i>a</i> -Si	Present work (TBMD)	149	46.9	55.4
<i>a</i> -Si	SW from Ref. 8	152	86.2	32.9

with respect to the strain tensor  $\epsilon_{kl}$ . During a TBMD run  $\tau_{ij}$  is calculated as the ensemble average  $\tau_{ij} = \langle t_{ij} \rangle$  of the microscopic stress tensor<sup>6</sup>

$$t_{ij} = \frac{1}{V_0} \hat{S}_{(ij)} \sum_{\alpha} \left( -x_{\alpha,i} \frac{\partial U}{\partial x_{\alpha,j}} + \frac{1}{m_{\alpha}} p_{\alpha,i} p_{\alpha,j} \right), \quad (3)$$

where  $m_{\alpha}$  and  $\mathbf{p}_{\alpha}$  are the mass and the momentum of the  $\alpha$ th atom, respectively, and  $V_0$  is the equilibrium volume. Latin subscripts indicate Cartesian components. The action of the operator  $\hat{S}_{(ij)}$  on a second-rank tensor  $a_{ij}$  is defined as  $\hat{S}_{(ij)} a_{ij} = (a_{ij} + a_{ji})/2$ . In the present case, the ensemble average  $\langle t_{ij} \rangle$  is measured during a canonical TBMD run where the simulation box is fixed in shape (cubic cell) and its volume  $V_0$  is selected as to reproduce the experimental density (here assumed as the zero-stress condition).<sup>13,14</sup>

The strain derivative appearing in Eq. (3) is calculated following Ref. 11 and the final expression for  $C_{ijkl}$  is

$$C_{ijkl} = C_{ijkl}^{(\text{pot})} + C_{ijkl}^{(\text{kin})} + C_{ijkl}^{(\text{fluc})}, \quad (4)$$

where the potential, kinetic, and fluctuation contributions are given by

$$C_{ijkl}^{(\text{pot})} = \frac{1}{V_0} \hat{S}_{(ij)} \hat{S}_{(kl)} \sum_{\alpha, \beta} \left\langle x_{\alpha\beta,i} x_{\alpha\beta,k} \frac{\partial^2 \varphi}{\partial x_{\alpha\beta,j} \partial x_{\alpha\beta,l}} - \delta_{ik} x_{\alpha\beta,j} \frac{\partial \varphi}{\partial x_{\alpha\beta,l}} \right\rangle, \quad (5)$$

$$C_{ijkl}^{(\text{kin})} = \frac{4NK_B T}{V_0} \hat{S}_{(ij)} \hat{S}_{(kl)} \delta_{ik} \delta_{jl}, \quad (6)$$

$$C_{ijkl}^{(\text{fluc})} = -\frac{V_0}{K_B T} (\langle t_{ij} t_{kl} \rangle - \langle t_{ij} \rangle \langle t_{kl} \rangle) \quad (7)$$

( $K_B$  is the Boltzmann constant). Within the TBMD scheme the most demanding step is the calculation of the  $\partial \varphi / \partial x_{\alpha\beta,i}$  and  $\partial^2 \varphi / \partial x_{\alpha\beta,i} \partial x_{\alpha\beta,j}$  derivatives appearing in Eqs. (6)–(8) which must be computed numerically.

In order to test the accuracy of the present method, we have computed room-temperature EC's of *a*-Si as obtained by quenching from the melt. We used the same *a*-Si sample studied in Ref. 13, whose structural and electronic properties were found to be in rather good agreement with both experimental data and first-principles calculations. As for the vibrational spectrum, a rather good agreement with experimental data was found in the acoustic part (i.e., that portion relevant to the elastic properties), while a poorer agreement (25% disagreement) was obtained for the optical phonons.<sup>15</sup> The results are shown in Table I and have been obtained after a simulation as long as 48 ps, preceded by 2 ps of equilibration. We adopted a time step of  $10^{-15}$  s. Every  $C_{ij}$  elastic constant (Voigt notation) has been computed as the average of the three symmetry-equivalent components of the elastic tensor. In Table I we also report the results from a previous simulation based on the Stillinger-Weber (SW) potential. The experimental constants have been deduced, according to Ref. 16, from the measurement of the velocity of the Rayleigh wave and from the experimental Young

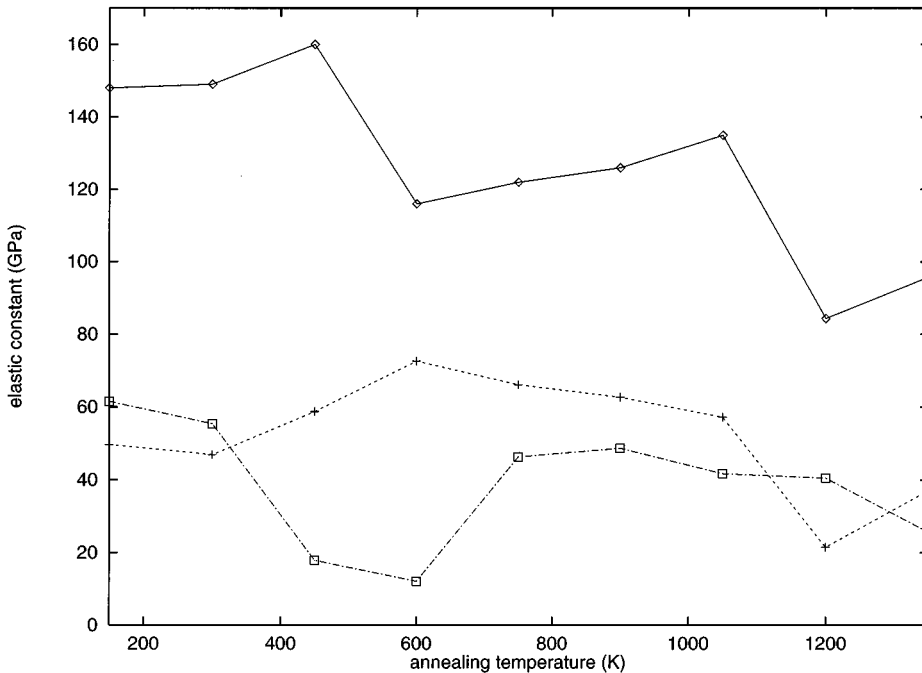


FIG. 1. Temperature dependence of EC's (units of GPa) in *a*-Si. Solid line,  $C_{11}$ ; dashed line,  $C_{12}$ ; dash-dotted line,  $C_{44}$ .

modulus.<sup>17</sup> We observe from Table I that the isotropy condition  $C_{11} - 2C_{44} = C_{12}$  is not well satisfied by our TBMD results. This is certainly due to the small system size (just 64 atoms). Despite that, the overall agreement of TBMD calculation with experimental data is quite good and much better than previous SW results. This is even more remarkable in view of the fact that no elastic properties have been inserted in the fitting data-base used to set up the TBMD scheme.<sup>18</sup> We also observe that all of the  $C_{ij}$ 's are significantly softened with respect to the crystalline case. In particular,  $C_{44}$  is decreased by about 30% and, therefore, it could be used as a parameter for monitoring the crystal-to-amorphous transition occurring during ion implantation. A number of simulations performed in the temperature range 150–1350 K has proved that EC's of *a*-Si are further decreased by heating the sample. The results are shown in Fig. 1. The trend is, however, not monotonous. We attribute such a feature to the metastability of the amorphous network. The Si structure undergoes temperature-induced lattice rearrangements which, in turn, affect the elastic properties of the sample. We prove that in Fig. 2 where we report the time-averaged value of the fluctuation term [Eq. (7)] of the nine components of the elastic tensor related to  $C_{11}$ ,  $C_{12}$ , and  $C_{44}$  and the mean square displacement (MSD) of Si atoms (bottom panel), as measured during a  $T=600$  K simulation. Lattice relaxations (marked by the LR label) always correspond to discontinuities in the time-averaged value of the elastic tensor components. Even in this case, however, we observe a sizable deviation from the isotropy condition. In other words, thermal annealing itself cannot remedy to the small simulation cell size.

Having established the reliability and accuracy of our computational scheme, we have studied the evolution of the EC's in bulk Si against the insertion of self-interstitial atoms. Again, we made use of previously generated defected samples (see Ref. 14), where a full amorphization of the Si lattice at the highest defect concentration (60 self-interstitials). The  $T=0$  K limit of Eqs. (5)–(7) (Ref. 11) was used to compute zero-temperature EC's of implanted Si. The general trend observed is that the defect-induced crystal-to-amorphous transition drives a softening of the elastic constants. Our findings are summarized in Table II where EC's of three different implanted samples are reported. We observe a qualitatively different behavior for  $C_{12}$ ,  $C_{44}$ , and  $C_{11}$ . While  $C_{12}$  and  $C_{44}$  decrease monotonically with the increasing number of defects, for  $C_{11}$  such a trend is inverted when the concentration of self-interstitials is as large as that needed to drive the amorphization transition. The results on  $C_{12}$  and  $C_{44}$  are in qualitative agreement with indirect information coming from Brillouin scattering measurements.<sup>19</sup> This confirms our conclusion to consider  $C_{44}$  as the more suitable parameter for monitoring the amorphization transition. It is worth noting that the isotropy condition is again not well satisfied, despite the fact that a larger cell was used. We attribute that to the peculiar way we have inserted defects<sup>14</sup>, which unlikely provides an isotropic sample, and to the relatively short annealing time, which surely is not long enough to fully relax the implanted host.

Finally, we have investigated the effects of thermal annealing on the elastic properties of implanted silicon. The fully amorphized 276-atom sample has been annealed at

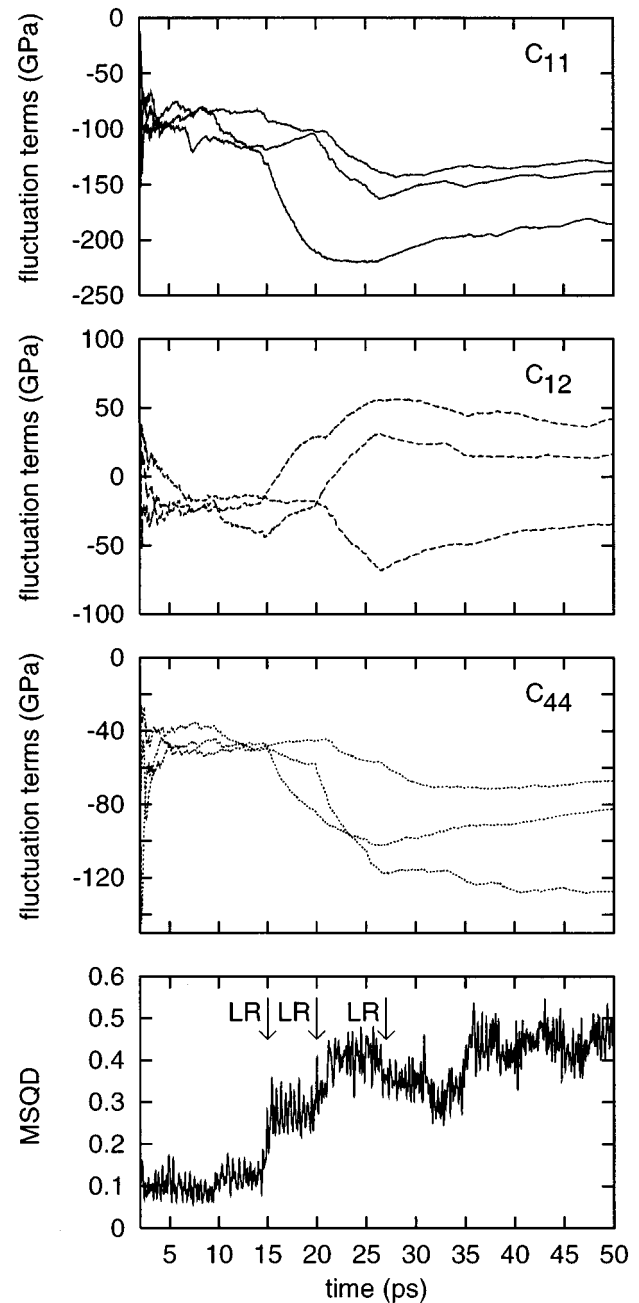


FIG. 2. Convergence of the fluctuation term [see Eq. (7)] of the isothermal elastic tensor for *a*-Si at  $T=600$  K. Solid, dashed, and dotted lines represent, respectively, the symmetry-equivalent components corresponding to the  $C_{11}$ ,  $C_{12}$ , and  $C_{44}$  elastic constants. In the bottom panel the mean square displacement (MSD) of Si atoms is shown (units of  $\text{\AA}^2$ ). Lattice relaxations (LR's) are marked by arrows.

three different maximum temperatures: 450, 600, and 750 K using the same heating/cooling rate.<sup>14</sup> The EC's have been computed in the  $T=0$  K limit. Results are shown in Table III. The annealing at the lower temperatures (450 K and 600 K) leaves the elastic constants practically unchanged with a minor trend towards a further decrease with respect to the crystalline case. Conversely, we observe a reverse trend when annealing up to  $T=750$  K: Here all of the elastic constants are increased. This result is related to the better struc-

TABLE II. Zero-temperature elastic constants (units of GPa) of defected silicon. The defect concentrations of 9.3%, 13.9%, and 27.8% correspond, respectively, to 20, 30, and 60 self-interstitial atoms randomly inserted into a 216-atom simulation box (see Ref. 14).

Defect concentration	$C_{11}$	$C_{12}$	$C_{44}$
9.3%	168	88.3	77.8
13.9%	163	82.2	74.4
27.8%	172	76.6	67.1

tural quality of the sample annealed at 750 K. As a matter of fact, in Ref. 14 we computed the atomic coordination of the annealed network and we found that the number of under-coordinated or over-coordinated sites was reduced. In other words, the partial recovering of the crystal order is followed by an overall hardening of the structure.

In conclusion, we proved that TBMD simulations can be successfully applied to investigate finite-temperature elastic properties of defected and amorphous semiconductors. We have monitored the evolution of EC's towards an overall softening during a crystal-to-amorphous transition as observed either during ion implantation and during cooling from the melt. In both cases, the parameter for the transition

TABLE III. Zero-temperature elastic constants (units of GPa) of  $\alpha$ -Si as function of the maximum temperature of the post-implantation annealing (see Ref. 14).

Annealing temperature	$C_{11}$	$C_{12}$	$C_{44}$
No annealing	172	76.6	67.1
450 K	174	76.6	66.3
600 K	172	74.8	65.5
750 K	179	81.5	68.1

can be identified in the  $C_{44}$  constant. These results enlarge the range of quantum-mechanical computer simulations of materials properties.

### ACKNOWLEDGMENTS

We thank P. Ballone (Stuttgart), G. Benedek (Milano), and P. Mutti (Milano) for helpful discussions. One of us (G.D.S.) acknowledges partial financial support by the National Research Council (CNR) of Italy under Project "Progetto Finalizzato Materiali Speciali per Tecnologie Avanzate."

- 
- <sup>1</sup>G. Grimvall, *Thermophysical Properties of Materials* (North-Holland, Amsterdam, 1986).
- <sup>2</sup>A.B. Chen, A. Sher, and W.T. Yost, in *Semiconductor and Semimetals*, edited by R.K. Willardson and C. Beer (Academic, New York, 1992), Vol. 37.
- <sup>3</sup>S. Baroni, P. Giannozzi, and A. Testa, *Phys. Rev. Lett.* **59**, 1665 (1987).
- <sup>4</sup>O.H. Nielsen and R.M. Martini, *Phys. Rev. B* **32**, 3780 (1985).
- <sup>5</sup>J.E. Osburn, M.J. Mehl, and B. M. Klein, *Phys. Rev. B* **43**, 1805 (1991).
- <sup>6</sup>J.R. Ray, *Comput. Phys. Rep.* **8**, 109 (1988).
- <sup>7</sup>F.H. Stillinger and T.A. Weber, *Phys. Rev. B* **31**, 5262 (1985).
- <sup>8</sup>J. Tersoff, *Phys. Rev. B* **37**, 6991 (1988).
- <sup>9</sup>M.D. Kluge, J.R. Ray, and A. Rahman, *J. Chem. Phys.* **85**, 4028 (1986).
- <sup>10</sup>M.D. Kluge and J.R. Ray, *Phys. Rev. B* **37**, 4132 (1988).
- <sup>11</sup>J.F. Lutsko, *J. Appl. Phys.* **65**, 2991 (1989).
- <sup>12</sup>L. Colombo, in *Annual Review of Computational Physics*, edited by D. Stauffer (World Scientific, Singapore, 1996), Vol. 4; C.Z. Wang and K.M. Ho, *Comput. Mater. Sci.* **2**, 93 (1994).
- <sup>13</sup>G. Servalli and L. Colombo, *Europhys. Lett.* **22**, 107 (1993).
- <sup>14</sup>L. Colombo and D. Maric, *Europhys. Lett.* **29**, 623 (1995).
- <sup>15</sup>G. Servalli and L. Colombo (unpublished).
- <sup>16</sup>J. Zuk *et al.*, *J. Appl. Phys.* **73**, 4951 (1993); X. Jiang *et al.*, *ibid.* **69**, 3053 (1991).
- <sup>17</sup>S.I. Tan, B.S. Berry, and B.L. Crowder, *Appl. Phys. Lett.* **20**, 88 (1972).
- <sup>18</sup>L. Goodwin, A.J. Skinner, and D.G. Pettifor, *Europhys. Lett.* **9**, 701 (1989).
- <sup>19</sup>B. Bhadra, J. Pearson, P. Okamoto, L. Rehn, and M. Grimsditch, *Phys. Rev. B* **38**, 12 656 (1988).